Journal of
Plankton Research

plankt.oxfordjournals.org

J. Plankton Res. (2016) 38(5): 1163–1177. First published online August 16, 2016 doi:10.1093/plankt/fbw052

The influence of nitrogen inputs on biomass and trophic structure of ocean plankton: a study using biomass and stable isotope size-spectra

CARMEN MOMPEÁN[1], ANTONIO BODE[1]*, MIKEL LATASA[2], BIEITO FERNÁNDEZ-CASTRO[3], BEATRIZ MOURIÑO-CARBALLIDO[3] AND XABIER IRIGOIEN[4,5]

[1]INSTITUTO ESPAÑOL DE OCEANOGRAFÍA, CENTRO OCEANOGRÁFICO DE A CORUÑA, APDO. 130, E15080 A CORUÑA, SPAIN, [2]INSTITUTO ESPAÑOL DE OCEANOGRAFÍA, CENTRO OCEANOGRÁFICO DE GIJÓN/XIXÓN, AVDA. PRÍNCIPE DE ASTURIAS 70BIS, E33212 GIJÓN/XIXÓN, SPAIN, [3]DEPARTAMENTO DE ECOLOGÍA Y BIOLOGÍA ANIMAL, UNIVERSIDAD DE VIGO, E36310 VIGO, SPAIN AND [4]AZTI, ARRANTZA ETA ELIKAIGINTZARAKO INSTITUTU TEKNOLOGIKOA, HERRERA KAIA PORTUALDEA, 20110 PASAIA, SPAIN

[5]PRESENT ADDRESS: KING ABDULLAH UNIVERSITY OF SCIENCE AND TECHNOLOGY [KAUST], RED SEA RESEARCH CENTER, THUWAL 23955-6900, SAUDI ARABIA

*CORRESPONDING AUTHOR: antonio.bode@co.ieo.es

Received March 9, 2016; accepted June 14, 2016

Corresponding editor: Roger Harris

Large scale patterns in planktonic food web structure were studied by applying continuous size-scaled models of biomass and $\delta^{15}N$ to plankton samples, collected at 145 stations during the Malaspina-2010 Expedition across three ocean basins and including major biomes. Carbon biomass and $\delta^{15}N$ were determined in size-fractionated samples (40 to 5000 μm) collected by vertical hauls (0–200 m). Biomass-normalized size-spectra were constructed to summarize food web structure and spatial patterns in spectral parameters were analyzed using geographically-weighted regression analysis. Except in the northwestern Atlantic, size-spectra showed low variability, reflecting a homogeneity in nitrogen sources and food web structure for the central oceans. Estimated predator-to-prey mass ratios <104 and mean trophic transfer efficiency values between 16% (coastal biome) and >20% (Trades and Westerlies biomes) suggested that oceanic plankton food webs may support a larger number of trophic levels than current estimates based on high efficiency values. The largest changes in spectral parameters and nitrogen sources were related to inputs of atmospheric nitrogen, either from diazotrophic organisms or dust deposition. These results suggest geographic homogeneity in the net transfer of nitrogen up the food web.

KEYWORDS: stable isotopes; $\delta^{15}N$; plankton; ocean; food web; biomass; size spectrum

available online at www.plankt.oxfordjournals.org

INTRODUCTION

Ocean plankton is an essential contributor to the dynamics of the earth climate system. Phytoplankton drawdown of CO_2 depends on nutrients such as nitrogen, and the fate of the organic matter produced depends on the characteristics of the food web, that in turn are largely determined by the size of planktonic organisms (Legendre and Le Fèvre, 1995). The effects of warming and increasing stratification imply reductions in the input of nutrients from deep waters to the surface ocean and subsequent changes in primary production in large ocean areas (Behrenfeld *et al.*, 2006). Depending on the structure of the food web the climate effects can be amplified or modified as shown by both *in situ* (Richardson and Schoeman, 2004) and modeling studies (Chust *et al.*, 2014). Thus, determining the structure of the food web is essential for understanding the behavior of ocean ecosystems under a changing climate.

Based on the dependency of most physiological processes on organism size, models relating organism abundance (or biomass) and individual size have been developed with the aim of describing the continuous change of biomass across the whole food web (Platt and Denman, 1978; Blanco *et al.*, 1994). The so-called size-spectrum models have been used to synthesize the food web structure in comparative analysis of oceanic ecosystems (Rodriguez and Mullin, 1986; Piontkovski *et al.*, 2003; Quiñones *et al.*, 2003; San Martin *et al.*, 2006). Furthermore, they have been used to infer the maximum number of trophic levels (NTL) that a particular ecosystem can support (Zhou, 2006; Basedow *et al.*, 2010). Their applicability has been questioned as their predictions generally require steady state conditions and uniformity in the size-dependent physiological rates (Poulin and Franks, 2010), but some of these limitations can be overcome by models (Ward *et al.*, 2014) or the use of seasonal averages (Hunt *et al.*, 2015).

Stable isotope analysis provides an important tool for elucidating trophic structure. For instance, enrichment in ^{15}N has been observed with increasing trophic position, thus allowing trophic structure to be inferred (e.g. Post, 2002). This enrichment can also be expected across plankton size classes, as pelagic food webs are strongly size-structured, the smallest organisms being generally primary producers and large organisms consumers of smaller prey (Platt and Denman, 1978). However, only a few field studies have explored the implications of the variability in ^{15}N with plankton size (Fry and Quiñones, 1994; Rolff, 2000; Bode *et al.*, 2007; Jennings *et al.*, 2008; Mompeán *et al.*, 2013). One of the main limitations has been the difficulty in obtaining measurements over a large number of size classes representative of the different trophic levels. The adjustment of simple continuous functions is not always possible because of the frequent exceptions to the general increase of ^{15}N with the average size of the organisms sampled size. For instance, plankton of total length smaller than 200 μm tend to show lower variability in average ^{15}N content than plankton in larger size classes (Rolff, 2000; Bode *et al.*, 2007). This is due both to the high variability at short time scales in small size classes owing to fast turnover times, thus reflecting rapid changes in the N sources (e.g. Jennings *et al.*, 2008), but also to the small changes in isotopic composition observed in microbial food webs (e.g. Gutiérrez-Rodríguez *et al.*, 2014). In addition, the presence of large or colonial plankton that feed on phytoplankton cause a decrease in ^{15}N at large sizes, while there is a linear increase with plankton size when these large herbivores are not present (Fry and Quiñones, 1994; Hunt *et al.*, 2015). Besides, because most studies have used net sieves with a logarithmic increase in mesh size, the direct comparison of ^{15}N content with size did not allow for the computation of significant linear functions in some of the samples, even when considering a relatively large range of sizes (e.g. Rolff, 2000). As for the biomass distributions, the use of logarithmic transformations and normalization of the variable of interest (^{15}N in this case) by the biomass of the organisms may lead to the construction of size-spectra that allow inferences on the trophic structure of plankton independently of the actual range of sizes measured. To our knowledge, this study represents the first application of biomass-normalized size spectra using stable isotopes.

Large regions of the open ocean are poorly sampled. Here, food webs are generally characterized by low nutrient concentrations, low biomass and dominance of microbial recycling of nutrients with some exceptions due to external nutrient supply (Longhurst, 2007). Studies analyzing planktonic size structure at large oceanic scales are scarce (Piontkovstki et al., 2003; Quiñones *et al.*, 2003; San Martin *et al.*, 2006) while there are no studies addressing the changes of stable nitrogen isotopes with plankton size at such scales. Meta-analyses of planktonic isotopic composition in plankton at large geographic scales have shown latitudinal patterns that were related to the sources and bioavailability of nutrients (Bowen, 2010; McMahon *et al.*, 2013). In this study we use biomass and ^{15}N size spectra to assess whether the type of dominant source of inorganic nutrients affects the trophic structure of plankton in the open ocean. The underlying hypothesis is that the trophic structure of plankton will be determined by the balance between nutrient inputs from deep or continental waters or from the atmosphere. Advective inputs can

be expected to be of importance at relatively small spatial or temporal scales, such as those related to mesoscale dynamics (Oschlies and Garçon, 1998), while most of the nutrients for the oligotrophic ocean are provided by transport across the pycnocline (Mouriño-Carballido *et al.*, 2011; Torres-Valdes *et al.*, 2009; Fernández-Castro *et al.* 2015). Atmospheric inputs include biological N_2 fixation (Capone *et al.*, 2005; Mulholland, 2007) and deposition of inorganic and organic nutrients, the latter noticeably enhanced by anthropogenic emissions (Duce *et al.*, 2008). Advection of deep nutrients is expected to lead to blooms of phytoplankton of relatively large size, high primary production and metazoan food webs, typical of most temperate and polar regions, with a strong seasonal variability (Longhurst, 2007). Most of the open ocean is expected to depend on non-seasonal, relatively small inputs of nutrients by diffusion, leading to phytoplankton of small size, low primary production and rapid remineralization of organic matter in microbial food webs. Atmospheric N fixation can be due to either large phytoplankton (such as the colony-forming cyanobacteria *Trichodesmium*) or to microbial forms, but in all cases low primary production and high microbial remineralization is expected before effective transfer of the fixed N up the food web (Mulholland, 2007). Because of the dependence of N fixation on micronutrients, such as Fe provided by dust deposition (Moore *et al.*, 2009), atmospheric inputs of nutrients may have also a clear seasonal component. In all cases, the trophic structure of the food web will depend on the net amount of nutrients transferred from the primary producers to the various types of consumers. This implies, by assuming a constant transfer efficiency between trophic levels (Zhou, 2006), that most of the oligotrophic open ocean would have shorter food webs than productive seasonal regions, as the biomass of pelagic predators depends on the amount of primary production (Chassot *et al.*, 2007). However, a larger number of trophic steps is expected in the oligotrophic ocean because of the rapid recycling of organic matter in microbial food webs (Sommer *et al.*, 2002).

The objective of this study is to investigate the relationships between plankton trophic structure and the source of N at large-scale spatial scales. For this purpose we analyzed carbon biomass and the natural abundance of stable nitrogen isotopes in a large set of size-fractionated plankton samples from the research expedition Malaspina-2010 across three ocean basins.

METHOD

Plankton sampling and analysis

Plankton samples were collected during Malaspina-2010 expedition between December 2010 and July 2011 (Fig. 1). The expedition employed two oceanographic ships to make observations and collect water, seston and plankton samples across three major ocean basins (http://metamalaspina.imedea.uib-csic.es/geonetwork/srv/en/main.home). In this study plankton samples from 145 stations were considered. Samples were collected by vertical hauls of bongo-type nets (30 cm diameter, 40 μm mesh size and 50 cm diameter and 200 μm mesh size) between 200 m depth and the surface during early morning. Plankton was size-fractionated using sieves of 200, 500, 1000, 2000 and 5000 μm, collected on pre-weighted glass-fiber filters and oven dried (60°C, 24 h) on board. Large gelatinous organisms were removed and analyzed separately (Molina-Ramírez

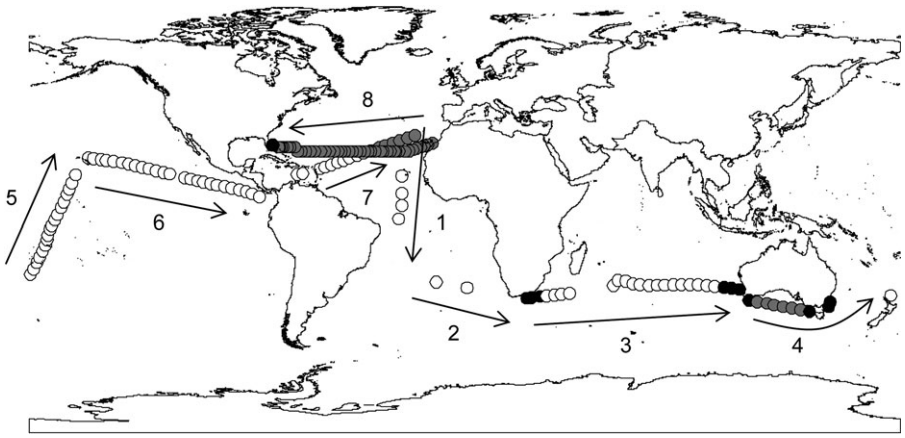

Fig. 1. Position of stations sampled during the Malaspina-2010 expedition for determination of size-fractionated plankton biomass and natural abundance of stable nitrogen isotopes. The colors indicate the biomes (black: Coastal, gray: Westerlies, white: Trades) according to Longhurst (2007). The arrows and numbers indicate the different cruise legs and track direction.

et al., 2015). In addition, sample aliquots were preserved in formalin (4% final concentration) for later determination of the abundance of trichomes of the N-fixing cyanobacterium *Trichodesmium*. Counts were made using a semiautomatic image analysis flow-through system (FlowCam).

Biomass was later determined in the laboratory for each size fraction as carbon (C) and nitrogen content using an elemental analyzer (Carlo Erba CHNSO 1108). No acidification treatment to remove carbonates was applied prior to analysis of carbon, but molar C:N values (mean ± SE = 4.8 ± 1.39, $n = 145$) were typical of planktonic organic matter (Søreide *et al.*, 2007) and indicated that the possible overestimation of C due to inorganic carbon would be small. Natural abundance of stable nitrogen isotopes was determined using a mass spectrometer (Finnigan Mat Delta Plus) coupled to the elemental analyzer. Nitrogen stable isotope abundance were expressed as $\delta^{15}N$ (‰) relative to atmospheric nitrogen (Coplen, 2011). International Atomic Energy Agency USGS40 and L-alanine isotope standards were analyzed with the samples, along with internal acetanilide and sample standards. Precision (±SE) of replicate determinations of standards and samples was <0.1‰ ($n = 2$ to 6) and <0.3‰ ($n = 5$ to 10), respectively. The analytical offset between certified and measured values was <0.1‰. All isotopic determinations were made in the Servicio de Análisis Instrumental of the Universidade da Coruña (Spain). Further details on the sampling and analysis can be found in Moreno-Ostos (2012) and Mompeán *et al.* (2013).

Oceanographic conditions *in situ*

Hydrographic information was obtained from CTD-rosette casts at the same stations and chlorophyll-a (Chl*a*) was determined from acetone extracts of phytoplankton collected at up to eight discrete depths in the photic layer (>0.1% of surface photosynthetically active irradiance). Here Chl*a* values were integrated in the photic layer as a proxy for phytoplankton biomass. In addition, the vertical extent of phytoplankton was estimated by the depth of the chlorophyll maximum (DCM). As nutrient concentrations and fluxes were not available for all the sampled stations (Fernández-Castro *et al.*, 2015), several proxies for nutrient supply from deep waters were employed. First, the DCM itself, as it was negatively correlated with the flux of nitrate (Fig. 1S). Second, the stratification of the upper water column (Behrenfeld *et al.*, 2006). estimated by the mixing layer depth (MLD), computed using a density difference criterion ($\Delta\delta = 0.125\,\mathrm{kg\,m^{-3}}$ with respect to surface values), and the mean squared Brunt–Väisälä frequency (N^2) values computed at 1 m intervals for the upper 200 m. Additional details on the sampling and on the analytical methods employed can be found in Moreno-Ostos (2012).

Satellite observations

As the observed plankton properties (i.e. biomass, stable isotopes) at each station would be the consequence not only of local conditions but also of general oceanographic conditions prevailing over a wider range of space and time, additional variables, estimated from satellite observations, were also considered. Annual averages of primary production for 2010 (PP, mg C m^{-2} d^{-1}) were generated by averaging monthly data for primary production downloaded from the Ocean Productivity website (http://www.science.oregonstate.edu/ocean.productivity/index.php) from the grid (0.17° × 0.17°) closest to each station position.

Dust deposition, as a proxy for atmospheric inputs of key nutrients for primary production (e.g. Fe or P), was also estimated from Aqua-MODIS Aerosol Optical Depth at 550 nm and Aerosol Small Mode Fraction data provided by the Giovanni online data system (NASA Goddard Earth Sciences). These data were retrieved from a grid of 1° resolution and centered at the closest location to each station and combined with wind speed derived from AVISO (http://las.aviso.oceanobs.com/las/getUI.do) to estimate the monthly average atmospheric dust column concentration (MDU, g m^{-2}) at each station (Kaufman *et al.*, 2005).

Creation of size spectra

Biomass and $\delta^{15}N$ values by size fractions of plankton were combined in the form of linear regressions with the median size of individuals in the corresponding size fraction. This median size was estimated as the geometric mean of the nominal size (length) of the sieves employed for each class, and further calculation of carbon biomass by using conversion factors (Rodriguez and Mullin, 1986). Due to the large variability in the values, a single regression including all stations sampled was not possible (Fig. 1S). Logarithmic transformations ($\log_2$) and normalization by the width of the interval of individual biomass were applied to obtain functions independent from size-class width (Blanco *et al.*, 1994; Zhou, 2006). The resulting biomass-normalized lines (obtained by least squares regression) characterized the size distribution of biomass or $\delta^{15}N$ by two parameters: the intercept (C_a, $\delta^{15}N_a$), a proxy for the values in the first size class, and the slope (C_b, $\delta^{15}N_b$), indicative of the rate of change

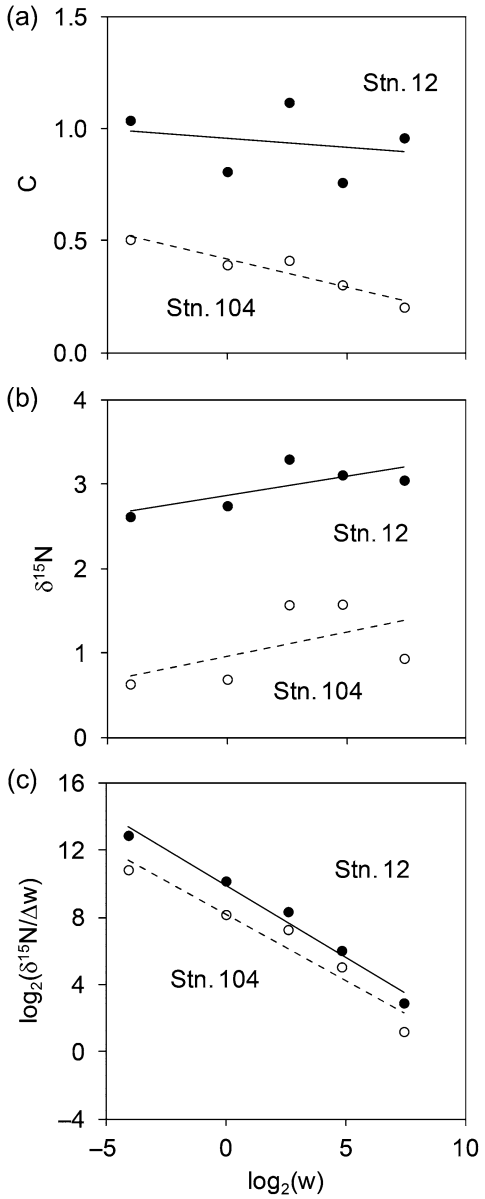

Fig. 2. Examples of size spectra for plankton samples collected at two stations of Leg 8 of the Malaspina-2010 expedition. (**a**) un-normalized spectra for biomass (C, mg m^{-3}), (**b**) un-normalized spectra for $\delta^{15}N$ (‰), (**c**) $\delta^{15}N$ biomass-normalized spectra. Mean biomass of the size class ($\log_2$(w)) in µg C.

in the values with increasing individual size (Fig. 2). Individual values of spectral regression parameters for each station are provided in the Supplement (Table IS). The normalization procedure can be reversed to obtain un-normalized values of the slope that can be further used to develop several descriptors of food web properties (Blanco *et al.*, 1994). For instance, we computed the NTL from C_b (Zhou, 2006), the predator-to-prey mass ratio (PPMR) from the slope m of the un-normalized $\delta^{15}N$ spectrum (Jennings *et al.*, 2001), and the trophic transfer efficiency (TTE) from PPMR (Barnes *et al.*, 2010). Where

$$\mathrm{NTL} = -(1 + 0.7)/(C_b 0.7)$$

by assuming a trophic efficiency (i.e. the ratio of production of predator to its prey) of 0.7 (Zhou, 2006),

$$\mathrm{PPMR} = 2^{2.2/m}$$

by assuming a $\delta^{15}N$ enrichment between trophic levels of 2.2‰, appropriate for plankton, ammonotelic organisms which show lower $\delta^{15}N$ enrichment than consumers excreting urea (Vanderklift and Ponsard, 2003; Hunt *et al.*, 2015), and

$$\mathrm{TTE} = \mathrm{PPMR}^{-1.05+0.75}$$

by assuming a time averaged un-normalized biomass slope of −1.05 (Barnes *et al.*, 2010; Hunt *et al.*, 2015).

In addition, the trophic position of the largest plankton size class (TP_{2000}) was computed from their $\delta^{15}N$ values ($\delta^{15}N_{2000}$) as

$$\mathrm{TP}_{2000} = \mathrm{TP}_{40} + \frac{\delta^{15}\mathrm{N}_{2000} - \delta^{15}\mathrm{N}_{40}}{2.2}$$

where TP_{40} is the trophic position of the 40–200 µm size class used as the reference baseline by assuming that it contained a mixture of phytoplankton and microzooplankton (TP_{40} = 1.5), and a constant $\delta^{15}N$ enrichment between adjacent trophic levels of 2.2‰ (Hunt *et al.*, 2015).

Spatial analysis

Stations were first grouped by biomes (Longhurst, 2007) (Fig. 1) to investigate large scale differences in biomass and spectral parameters using ANOVA and Dunnett-C post hoc tests. Visualization and further analysis of trends at various spatial scales were made using the tools provided by the package Spatial Analysis in Macroecology (SAM V 4.0) which allowed mapping and computation of various spatial statistics from metrics descriptive of spatial autocorrelation to advanced spatial regression (Rangel *et al.*, 2010). Spatial autocorrelation of variables was analyzed by means of correlograms of the Moran's I coefficient computed for groups of samples (stations) of increasing spatial distance. The relationships between spectral parameters and environmental variables were investigated using principal components analysis (PCA) to determine the main correlations. Then, we selected the most

representative environmental variables to construct regression models explanatory of each of the spectral parameters at each station using Geographically Weighted Regression (GWR). This method, specifically designed to deal with spatial autocorrelation and lack of stationarity (Rangel *et al.*, 2010), was used to compute a series of local regressions, one for each station location, between the independent variable (i.e. spectral parameters) and the explanatory variables (i.e. selected environmental variables) taking into account the information from the surrounding stations weighted by a spatial function. In this case we used a moving spatial window with an adaptive Kernel of 15% of neighboring stations optimized using the Akaike's Information Criterion. The explanatory power of GWR (r^2) for each spectral parameter was in general higher than those of ordinary least squares, as measured by ANOVA tests (Rangel *et al.*, 2011).

RESULTS

Spatial distributions

Biomass and $\delta^{15}N$ showed an uneven distribution as illustrated by the maps for the 40–200 µm size-class (Fig. 3). In contrast, the values for the parameters characterizing biomass and $\delta^{15}N$ spectra showed in general low variability, resulting in a relatively homogeneous distribution at large spatial scales (Fig. 4, Fig. 3S). An exception was the Subtropical North Atlantic region (cruise legs 7 and 8), mostly in the Westerlies biome. Here, the intercepts for both biomass and $\delta^{15}N$ spectra (C_a and $\delta^{15}N_a$) reached in general lower values than in other regions, while the slopes (C_b and $\delta^{15}N_b$) showed high variability. This latter pattern is a response to the low ^{15}N values measured in the 40–200 µm size-class (Fig. 3) in the subtropical regions thus resulting in an overall negative correlation with latitude ($r = -0.507$, $P < 0.001$, $n = 145$). The geographic and temporal distribution of samples also affected these distributions in complex ways, as there were positive correlations between $\delta^{15}N_b$ and either latitude ($r = 0.331$, $P < 0.001$) or sampling date ($r = 0.202$, $P < 0.05$). When grouped by biomes, the differences were significant in the Westerlies (including the southern Australia region) for all parameters and variables, except for $\delta^{15}N_b$ (Table I). Thus, the lower biomass and $\delta^{15}N$ values at the base of the planktonic food web in the Westerlies biome (C_{40-200} and $\delta^{15}N_{40-200}$) affected the food web structure represented by size spectra.

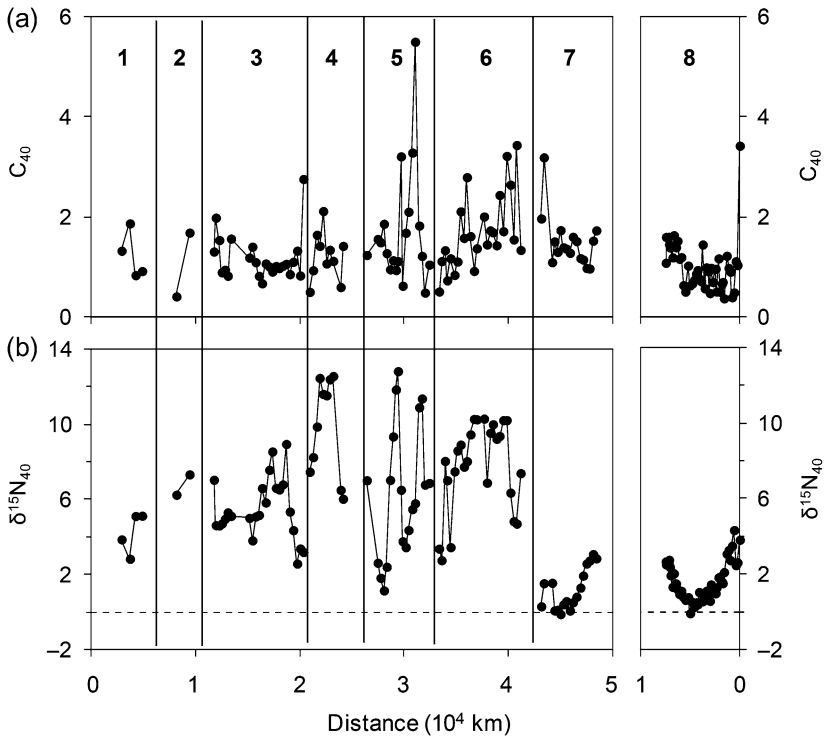

Fig. 3. Distribution of plankton biomass (**a**, C_{40}, mg C m^{-3}) and $\delta^{15}N$ (**b**, $\delta^{15}N_{40}$ ‰) in the 40–200 µm size fraction for stations sampled during the Malaspina-2010 expedition. The vertical dashed lines and numbers indicate the different cruise legs. The horizontal dashed line in b) indicates $\delta^{15}N = 0$. Note the inversion of values in the horizontal axis for Leg 8.

Table I: Mean ± SE values of the parameters of the size spectra for biomass (C_a: intercept; C_b: slope) and $\delta^{15}N$ ($\delta^{15}N_a$: intercept; $\delta^{15}N_b$: slope) and of carbon biomass ($C_{40–200}$, mg C m^{-3}) and $\delta^{15}N$ ($\delta^{15}N_{40–200}$, ‰) for the 40–200 μm size class in the three biomass sampled

Variable	Biome	Mean	SE	*n*	Group
C_a	Coastal	8.840	0.166	11	a
	Westerlies	7.954	0.095	55	b
	Trades	8.961	0.071	79	a
C_b	Coastal	−0.871	0.021	11	a
	Westerlies	−0.941	0.009	55	b
	Trades	−0.884	0.006	79	a
$\delta^{15}N_a$	Coastal	10.589	0.230	11	a
	Westerlies	9.444	0.163	55	b
	Trades	10.444	0.183	79	a
$\delta^{15}N_b$	Coastal	−0.867	0.008	11	a
	Westerlies	−0.824	0.010	55	a
	Trades	−0.832	0.012	79	a
C_{40}	Coastal	1.314	0.193	11	a
	Westerlies	1.083	0.068	55	a
	Trades	1.491	0.090	79	a
$\delta^{15}N_{40}$	Coastal	5.520	0.881	11	a
	Westerlies	2.723	0.422	55	b
	Trades	5.810	0.365	79	a

n, number of data. Means not significantly different are marked in the same group (ANOVA and Dunnett-C test, $P < 0.05$).

The trophic position of the largest plankton size-class sampled was significantly correlated with the slope of the $\delta^{15}N$ spectra (Fig. 4S) and reached values generally below 2, particularly for the samples in the coastal biome (Table II). In contrast, estimates using the biomass spectra resulted in a maximum number of ca. three trophic levels. Mean values of PPMR were below 1000 and no significant differences were found between biomes, while mean TTE was 16% for the coastal biome and >20% for the Trades and Westerlies biomes (Table II).

The distribution of annual primary production (Fig. 3S, f) was also quite homogeneous across the regions sampled, while variables indicative of different nutrient inputs, such as the abundance of *Trichodesmium*, the DCM or the atmospheric dust deposition were more heterogeneously distributed (Fig. 5, Fig. 3S). *Trichodesmium* was present in all regions but showed in general high values in the North Atlantic (Legs 7 and 8). The chlorophyll maximum was deepest in the central regions of all ocean basins. The distribution of other variables as the depth of the mixing layer or the Brunt–Väisälä frequency (not shown) was also variable at intermediate and large spatial scales but otherwise they were significantly correlated with the DCM ($r = -0.355$, $P < 0.01$, $n = 137$). Relatively high dust deposition was estimated in the North Pacific and in the North Atlantic, but in the latter there were large differences between the values corresponding to different cruise legs in this region. For instance, the largest dust deposition corresponded to the spring-summer leg and the lowest to the winter leg (Fig. 5c, Fig. 3S g).

Correlations of spectral and other variables

We found a correlation between the intercepts of each spectrum type (biomass or $\delta^{15}N$) and the values measured at the smallest size class (40–200 μm), as expected. There was also a negative correlation between the slopes of biomass and $\delta^{15}N$ spectra. All these correlations can be characterized by the angle between vectors in the space of the two main components of the PCA, explaining 46.3% of total variance (Fig. 6). The negative correlations between $\delta^{15}N_a$ and the DCM and the abundance of *Trichodesmium*, and the positive correlations between C_a and chlorophyll and primary production should be highlighted. In turn, $\delta^{15}N_b$ showed positive correlation with mean dust deposition and DCM while C_b was negatively correlated with DCM. Interestingly, DCM can be considered a better index of nutrient inputs across the thermocline than the MLD, as it was positively correlated with MLD and also with chlorophyll-*a*, primary production, biomass and $\delta^{15}N$ of the 40–200 μm size-class.

GWR models

From the global correlation and PCA results we selected the independent variables DCM (as an index of the vertical transport of nutrients across the thermocline), *Trichodesmium* abundance (as a proxy for atmospheric nitrogen fixation) and MDU (as a proxy for other atmospheric nitrogen inputs) to construct regression models explanatory of the spectral parameters (C_a, C_b, $\delta^{15}N_a$, $\delta^{15}N_b$) at local scale using GWR models (Table III). Most GWR models were significant ($P < 0.001$) and only the GWR model for C_b was non-significant ($P = 0.070$) and with less explanatory power than ordinary least squares (the latter with a relative decrease of 33.035 in the Akaike Information Criterion). The spatial autocorrelation of spectral variables and residuals indicated by Moran's I values (Fig. 7) showed that the spatial structure was better represented at all spatial scales in the case of $\delta^{15}N$ models, with lower residuals than models for biomass. The median values of the model parameters indicated that the distribution of the dependent variables was determined mainly by a constant value modulated by the coefficients of the

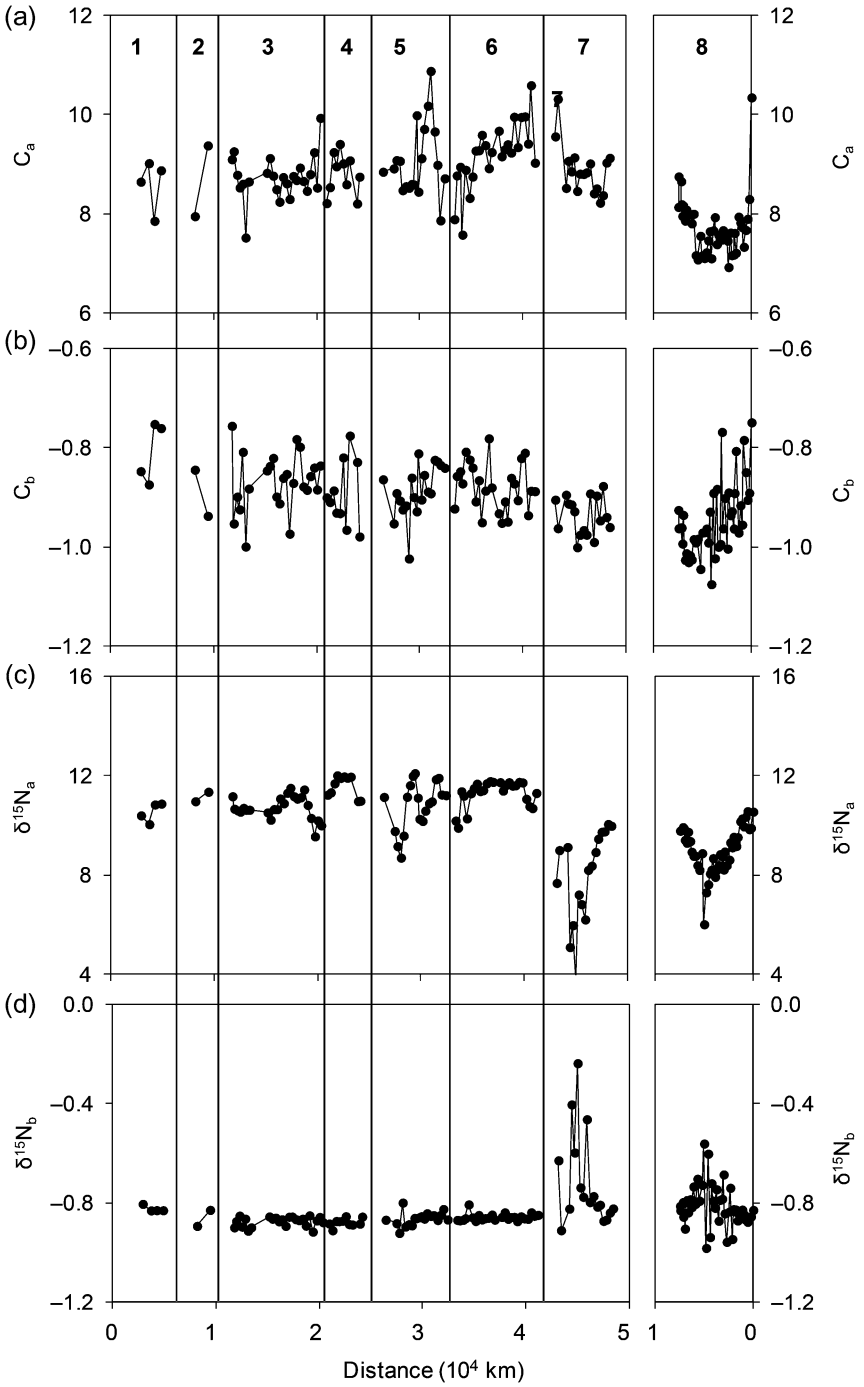

Fig. 4. Distribution of parameters of biomass (**a**, **b**) and $\delta^{15}N$ (**c**, **d**) plankton size spectra computed for stations sampled during the Malaspina-2010 expedition. (a, b): intercept of biomass (C_a) and $\delta^{15}N$ ($\delta^{15}N_a$) spectra, respectively. (c, d): slope of biomass (C_b) and $\delta^{15}N$ ($\delta^{15}N_b$) spectra, respectively. Cruise legs indicated as in Fig. 3.

independent variables (Table III). *Trichodesmium* abundance and DCM had marginal influence in general (median values close to 0) but their range of values indicated some local influence. In contrast, median values for MDU coefficients ranked second after the constant values, suggesting that this variable was important for determining the shape of $\delta^{15}N$ spectra and the biomass at the base of the food web (C_a).

Table II: Mean ± SE values of the trophic position of the 2000–5000 μm size-class (TP_{2000}) and food web parameters derived from size spectra in the three biomass sampled

Variable	Biome	Mean	SE	*n*	Group
TP_{2000}	Coastal	1.47	0.12	11	b
	Westerlies	1.91	0.07	55	a
	Trades	1.95	0.07	79	a
NTL	Coastal	2.81	0.07	11	a
	Westerlies	2.60	0.03	55	b
	Trades	2.76	0.02	79	a
PPMR	Coastal	696.71	199.75	11	a
	Westerlies	378.49	148.22	55	a
	Trades	723.12	203.19	79	a
TTE	Coastal	16.44	1.55	11	b
	Westerlies	24.91	1.72	55	a
	Trades	21.66	1.42	79	a, b

NTL, number of trophic levels (Zhou, 2006); PPMR, predator-to-prey mass ratio (Jennings *et al.*, 2001); TTE, trophic transfer efficiency, as % (Barnes *et al.*, 2010); n, number of data. Means not significantly different are marked in the same group (ANOVA and Dunnett-C test, $P < 0.05$).

DISCUSSION

The results of this study showed that the size spectra of stable nitrogen isotopes add a new dimension to characterizing the structure of oceanic planktonic food webs. The parameters defining the size spectrum in each particular region were correlated with the main sources of nutrients for primary production, such as the vertical transport across the thermocline and atmospheric inputs. Thus, the use of stable isotope spectra complement the information provided by biomass spectra, which have already been established as an useful tool for describing and modeling the structure and function of pelagic ecosystems (Rodriguez and Mullin, 1986; Quiñones *et al.*, 2003; San Martin *et al.*, 2006; Zhou, 2006). The large number of observations collected across three ocean basins in our study suggests that the resulting relationships are of general application to all pelagic environments.

Isotope size-spectra in the central region of the ocean

The samples used in this study do not cover all possible oceanic conditions as most of the observations were made in central areas of the ocean. Also, temporal variability (e.g. seasonality) was not taken into account for most regions. However, three of the four ocean biomes were covered (only the polar biome was not included in the study), and the range of primary production values is representative of most of the open ocean, even including some data from the most productive upwelling regions (e.g. Benguela). In addition, the observations across the subtropical North Atlantic were made in two different seasons (winter-early spring and late spring-summer) thus providing some indications of temporal variability, at least in this region. This is supported by the overall correlations with the sampling date for either $\delta^{15}N40$ or $\delta^{15}N_b$. In agreement with the low relative importance of seasonality for plankton in the tropical and subtropical ocean (Longhurst, 2007), we found small differences in size-spectra in this region, even when there were large differences in dust inputs between transects made in different seasons (Fig. 5c, Fig. 3S g). Short term variability (e.g. those caused by diel migrations of plankton between deep and surface layers) is likely to have a small effect on our results as the sampling was conducted approximately at the same period of the day through all cruises.

The range of individual sizes considered could also influence the estimation of the parameters of the spectra (Blanco *et al.*, 1994). Besides, a large fraction of the primary production in the central regions of the ocean is due to phytoplankton cells much smaller than the sizes considered in our samples (Marañón, 2009). Although we employed only five discrete size-classes to construct the spectra, they included organisms ranging from 10 ng C to 0.5 mg C individual weight (i.e. four orders of magnitude). An inspection of some of the samples collected indicates a good representation of phytoplankton (including diatoms, dinoflagellates, phytoflagellates and cyanobacteria), and zooplankton filter-feeders and predators (Mompeán *et al.*, 2013). This wide range of organisms, along with the robust character of biomass-normalized size-spectra that allows for estimations of properties of the plankton community outside the actual range of fitted sizes (Blanco *et al.*, 1994), supports the validity of our estimations for the planktonic food web. In the case of $\delta^{15}N$, previous studies have shown that the spectra are continuous across the whole pelagic food web (Jennings *et al.*, 2001; Bode *et al.*, 2007; Barnes *et al.*, 2010; Hunt *et al.*, 2015).

Size-spectra and nutrient sources

When considering biome scales, our results show general homogeneity in the parameters defining the size spectra. Only the Westerlies biomes showed lower values of intercept and slope in the biomass spectra, and also lower intercept values of the $\delta^{15}N$ spectra, than those computed for the Trades and Coastal biomes. Such homogeneity in the size structure of the open ocean plankton can be interpreted in terms of the main controls of productivity. For most ocean regions, primary production is controlled by the availability of nutrients in the photic layer, and the main inputs

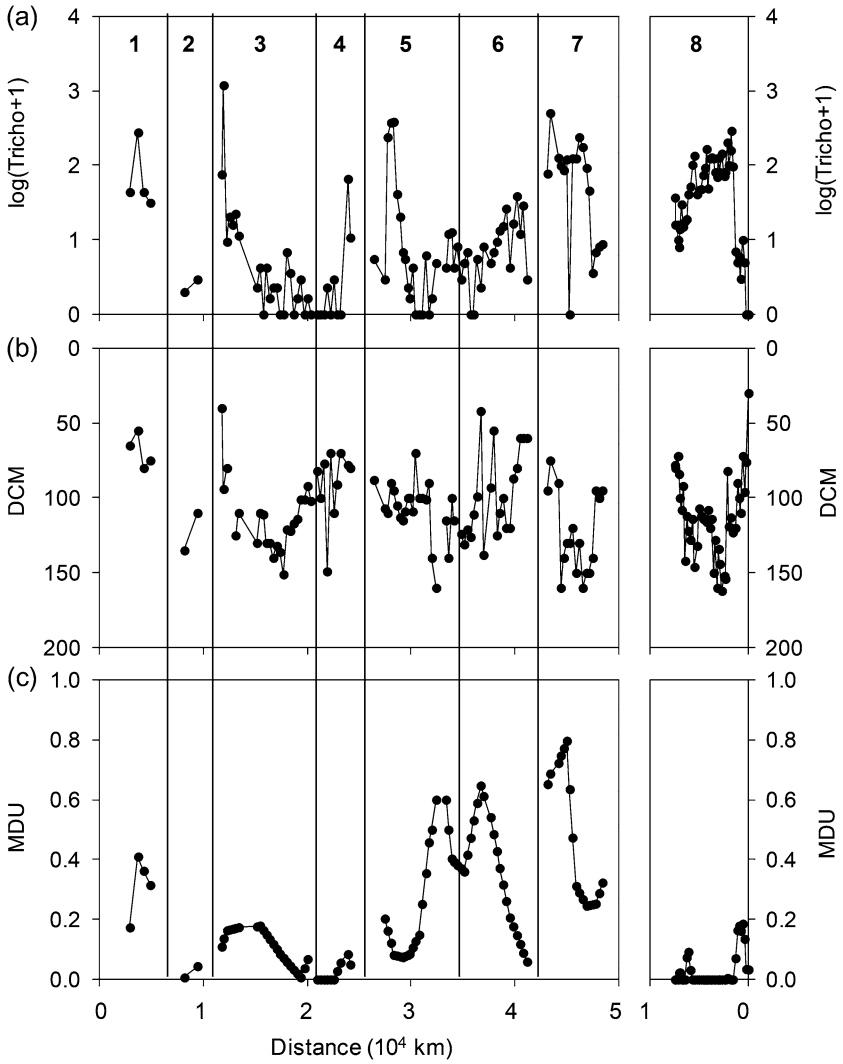

Fig. 5. Distribution of *Trichodesmium* abundance (**a**, Tricho, log (trichomes + 1) m^{-3}), depth of the chlorophyll maximum (**b**, DCM, m) and mean dust deposition (**c**, MDU, g m^{-2}) measured or estimated for stations sampled during the Malaspina-2010 expedition.

depend on eddy diffusion through the pycnocline (Fernández-Castro *et al.*, 2015) or advection of subsurface waters (Longhurst, 2007). These are likely the main fertilization mechanisms for the Trades and Coastal biomes, including productive upwelling in equatorial and coastal waters, while most of the subtropical oceans are occupied by oligotrophic gyres with reduced nutrient inputs and productivity (Behrenfeld *et al.*, 2006). Nevertheless, various mechanisms can provide local nutrient inputs, as mesoscale turbulence (Oschlies and Garçon, 1998), lateral transport from productive regions (Torres-Valdes *et al.*, 2009), atmospheric deposition (Duce *et al.*, 2008) and biological fixation of atmospheric nitrogen (Capone *et al.*, 2005). Notably, the subtropical North Atlantic is a region within the Westerlies biome where the fixation of nitrogen by diazotrophic plankton is favored by the deposition of Fe and phosphorus in dust particles (Capone *et al.*, 2005; Moore *et al.*, 2009; Fernández *et al.*, 2010). Notwithstanding the relatively small fixation rates recorded in tropical and subtropical waters of the South Atlantic, they also contributed to a large fraction of total nitrogen inputs when compared to those from eddy diffusion (Mouriño-Carballido *et al.*, 2011). Only in the vicinity of upwelling areas the contribution of deep water nitrogen produced a traceable $\delta^{15}N$ signal in plankton (e.g. Fernández *et al.*, 2010; Hauss *et al.*, 2013; Mompeán *et al.*, 2013) as observed in the increase of $\delta^{15}N_{40}$ from east to west in Legs 7 and 8 (Fig. 3).

Our results show how the importance of these fertilization mechanisms translates into a significant correlation between indices of different nutrient sources and

plankton biomass structure, the latter represented in this study by the parameters of the size spectra. Nutrient inputs from subsurface waters are indicated by the DCM, the layer where phytoplankton biomass accumulates because growth is maximized by a compromise between light levels (from above) and nutrient inputs (from below). The DCM, generally deeper when vertical advection/diffusion is low (e.g. at the center of oligotrophic gyres) and shallower when is high (e.g. near upwelling areas), also could be seasonally affected. Previous studies have revealed that the DCM is a better proxy for productivity than instantaneous nutrient concentrations in the surface layer (Mouriño *et al.*, 2004), and estimations of the vertical flux of nitrate during the Malaspina-2010 expedition (Fernández-Castro *et al.*, 2015) were significantly correlated with the DCM (Fig. 1S). In the case of atmospheric inputs, biological nitrogen fixation is generally associated to the abundance of the colony-forming *Trichodesmium*, although unicellular diazotrophs may be also important, as found in most of the studied stations across the North Atlantic (Benavides *et al.*, 2016). Dust deposition favors nitrogen fixation, as it provides the necessary additional micronutrients (Moore *et al.*, 2009; Fernández *et al.*, 2010), but it also introduces significant amounts of nitrogen and phosphorus (Morin *et al.*, 2009). Thus, the main nutrient inputs can be used to model the biomass at the base of the food web, represented in our model by C_a.

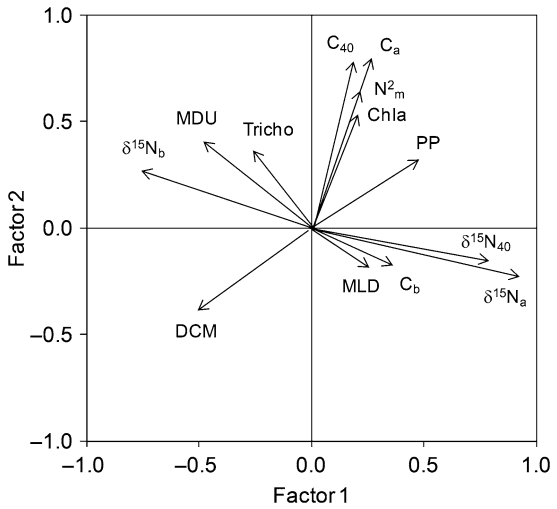

Fig. 6. Vectors of variables projected in the space of the two main components of the PCA. Factors 1 and 2 accounting for 39% and 18% of total variance, respectively. C_a and C_b, intercept and slope of the biomass spectra, respectively; $\delta^{15}N_a$ and $\delta^{15}N_b$, intercept and slope of the $\delta^{15}N$ spectra, respectively; PP, primary production; Tricho, *Trichodesmium* abundance; MDU, mean dust deposition; MLD, mixed layer depth; DCM, depth of the chlorophyll maximum; $C40$ and $\delta^{15}N_{40}$, biomass and $\delta^{15}N$ of the 40–200 µm size-class, respectively; Chl*a*, chlorophyll concentration; N^2_m, mean squared Brunt–Väisälä frequency.

Size-spectra and trophic structure

To our knowledge, this study represents the first application of biomass-normalized size spectra using stable isotopes. The increase in $\delta^{15}N$ with organism size is a general rule in pelagic food webs (Jennings *et al.*, 2001; Bode *et al.*, 2007; Jennings *et al.*, 2008; Barnes *et al.*, 2010; Hunt *et al.*, 2015). However, previous studies of $\delta^{15}N$ in different size classes of plankton failed to demonstrate a regular increase in $\delta^{15}N$ with size, as there were many exceptions both at large and small organism sizes (Fry and Quiñones, 1994; Rolff, 2000, Bode *et al.*, 2007; Landrum *et al.*, 2011, Mompeán *et al.*, 2013). The planktonic exception can be attributed to the presence of large herbivores (such as the colony-forming salps) but also to the different turnover times of biomass in organisms of different size (Jennings *et al.*, 2008). Besides, there is evidence of low or no enrichment in $\delta^{15}N$ within the microbial food web (Gutiérrez-Rodríguez *et al.*, 2014). The normalization procedure applied in this study overcomes the lack of a regular increase in each local spectrum computed with raw values, as in previous studies. The biomass-normalized spectrum allows for a synthetic representation of the continuous distribution of the variable of interest across organism sizes by using only two parameters (Zhou,

Table III: Median, minimum (min) and maximum (max) values of GWR coefficients for spectral parameters (C_a, $\delta^{15}N_a$ and $\delta^{15}N_b$) estimated from logarithmic Trichodesmium *abundance (Tricho, log trichomes m^{-3}), depth of chlorophyll maximum (DCM, m) and mean monthly dust deposition (g m^{-2} $month^{-1}$)*

	Constant			Tricho			DCM			MDU		
Dependent	Median	Min	Max	Median	Min	Max	Median	Min	Max	Median	Min	Max
C_a	9.162	5.842	12.391	0.001	−0.036	0.058	−0.002	−0.032	0.004	0.327	−5.685	7.134
$\delta^{15}N_a$	11.194	7.444	15.799	−0.004	−0.076	0.063	−0.002	−0.045	0.029	−2.416	−20.418	3.535
$\delta^{15}N_b$	−0.879	−1.473	−0.722	0.000	−0.003	0.004	0.000	−0.001	0.004	0.089	−0.088	0.682

All models were fit with $P < 0.05$ and include a constant term. Values from models for C_b are not shown as GWR was not significant for this variable.

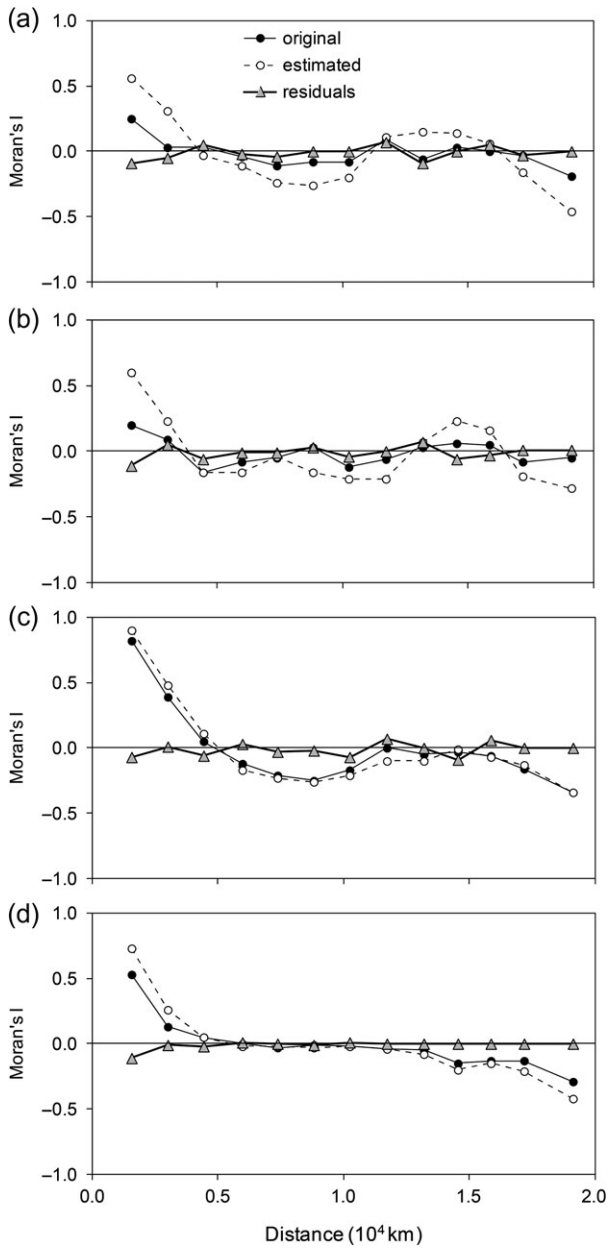

Fig. 7. Spatial autocorrelation (Moran's I) for spectral parameters estimated by GWR at different spatial scales. (**a**, **b**): C_a and C_b, intercept and slope of the biomass spectra, respectively; (**c**, **d**): $\delta^{15}N_a$ and $\delta^{15}N_b$, intercept and slope of the $\delta^{15}N$ spectra, respectively.

2006). Besides, the reversal in the normalization (Blanco *et al.*, 1994) facilitates the determination of the values of the un-normalized slopes employed in estimations of PPMR and TTE (Barnes *et al.*, 2010). Such un-normalized slopes cannot be obtained in a larger number of cases using raw values (e.g. Fig. 2S). In this study, changes in the intercept of the $\delta^{15}N$ spectrum were related to the dominant source of nitrogen for primary producers, while changes in the slope were indicative of the overall isotopic enrichment along the food web.

Low intercepts are thus expected in areas with significant atmospheric inputs, either from diazotrophy or by inputs of anthropogenic nitrogen, as these sources have $\delta^{15}N$ values near zero (Morin *et al.*, 2009). This was the case for our observations in the Westerlies biome that had lower $\delta^{15}N_a$ than the Trades and Coastal biomes (Table I), in agreement with the large importance of atmospheric nitrogen fixation in the former. However, we did not find significant differences in $\delta^{15}N_b$ between biomes and the detailed distribution of this parameter was very homogeneous (Fig. 4d). This suggests that the transfer of nitrogen up the planktonic food web proceeds, in general, at similar rates in all ocean regions. The exception was found for the two legs crossing the subtropical N Atlantic, where a large variability in $\delta^{15}N$ spectra was found in coincidence with relatively high amounts of *Trichodesmium* and other diazotrophs (Benavides *et al.*, 2016).

The relative homogeneity in the structure of oceanic plankton food webs suggested by $\delta^{15}N_b$ is supported by the low variability also observed in NTL, the latter independently estimated from C_b (Table II). On average, NTL indicated that the oceanic plankton food webs analyzed had <3 trophic levels, with maximum values in the Coastal and Trades biomes. These values are about one trophic level higher than the estimations of the trophic position for the largest plankton size class using $\delta^{15}N$. The difference would suggest that these planktonic food webs would support only one additional consumer level predating upon the largest size class analyzed. Some of consumers may well be the cnidaria and ctenophora removed from the largest size fraction of our samples, with estimated TP between 2.6 and 2.9 (Molina-Ramírez *et al.*, 2015). The trophic position of large plankton and the PPMR values obtained in our study are indicative of feeding on small plankton by most consumers. This is expected in oligotrophic waters dominated by picophytoplankton, (Hunt *et al.*, 2015), thus suggesting a common trophic structure related to the nutrient inputs. The resulting TTE values were in the range observed for pelagic (Hunt *et al.*, 2015) but also benthic ecosystems (Jennings *et al.*, 2001) indicating a relatively high efficiency in the transfer of energy through the food web. However, these values were lower than the average estimation of 70% for pelagic food webs (Zhou, 2006). For instance, using a global TTE average of 21% would increase the NTL to 6.4, thus suggesting that the use of biomass spectra corrected by a TTE estimate from $\delta^{15}N$ would take into account the larger number of trophic steps expected in oligotrophic waters (Sommer *et al.*, 2002).

The low variability observed in $\delta^{15}N$ slopes suggests that the overall trophic structure is similar across different planktonic communities, even when there are large variations in the nutrient sources and in the transmission of the energy through the food web. Organisms included in our spectra covered four orders of magnitude in individual size, implying large differences in growth rates and biomass turnover times, and thus greater variability in $\delta^{15}N$ composition of the small plankton versus large plankton (Jennings *et al.*, 2008). Such differences would explain the reported delays in the transmission of the $\delta^{15}N$ signal from the N source (e.g. atmospheric N) to zooplankton predators (Rolff, 2000; Mompeán *et al.*, 2013). The normalization procedure applied in our study overcomes the time-lags and local variability of $\delta^{15}N$ and, as normalized biomass spectra, provides a better tool to compare different communities than un-normalized spectra. Similarity in the $\delta^{15}N$ spectrum slopes and trophic structure across plankton communities can be expected if the underlying physiological processes are similar. Even when the nutrient (nitrogen) sources are different, the transmission up the food web is made by similar biochemical reactions for all planktonic communities. In the case of tropical and subtropical communities living in oligotrophic waters, recycling of dissolved organic matter through microbial communities is an important mechanism for transmission of nitrogen to upper trophic levels (Mulholland, 2007). The homogeneity in trophic structure across pelagic ecosystems was already suggested by the first studies of biomass and abundance size spectra (Platt and Denman, 1978) and confirmed by subsequent studies including upper trophic levels (Hunt *et al.*, 2015). Now, the application of biomass-normalized $\delta^{15}N$ spectra to whole food webs, including fish and upper consumers, can be used to analyze their variability by considering nitrogen exchanges.

CONCLUSIONS

Biomass and $\delta^{15}N$ size-spectra of plankton in general showed low variability, reflecting a large homogeneity in nitrogen sources and food web structure for the central oceans. The largest changes in spectral parameters and nitrogen sources were observed in the northwestern Atlantic and were related to inputs of atmospheric nitrogen, either from diazotrophic organisms or dust deposition. Mean PPMR between 4 and 3×10^3 were estimated for all biomes, while mean TTE values varied between 16% (coastal biome) and >20% (Trades and Westerlies biomes), thus suggesting that current estimates of the NTL based on a high average community efficiency may be too low, at least for most of the oligotrophic ocean. Both $\delta^{15}N$ and biomass size-spectra suggest geographic homogeneity in the net transfer of nitrogen up the food web.

SUPPLEMENTARY DATA

Supplementary data can be found online at http://plankt.oxfordjournals.org.

DATA ARCHIVING

The biomass and stable isotope data used in this paper was deposited in the Malaspina-2010 repository and can be accessed through the following links:

http://metamalaspina.imedea.uib-csic.es:80/geonetwork?uuid=91b1175d-894c-4e48-980f-9cc325dcd79e

http://metamalaspina.imedea.uib-csic.es:80/geonetwork?uuid=4f79814e-ebab-4e0f-aea9-25c88bacd25a

Data from Leg 8 are also available at the PANGAEA repository:

https://doi.pangaea.de/10.1594/PANGAEA.816451

ACKNOWLEDGEMENTS

We are grateful to all participants in the cruise legs for their collaboration in plankton sampling, to A.F. Lamas (IEO) for preparing samples for stable isotope analysis, to P. Chouciño and A. Fernández (UVigo) for assistance with the computation of dust deposition, to J. Lorenzo, J. Varela and M. Varela (IEO) for *Trichodesmium* counts, and to M. Estrada for useful comments to a first version of manuscript.

FUNDING

Malaspina-2010 (CSD2008-00077) funded by program CONSOLIDER-INGENIO 2010; Ministerio de Ciencia e Innovación (Spain), project EURO-BASIN (FP7-ENV-2010 264933) of the EU; Instituto Español de Oceanografia (IEO); PFPI (grant of IEO) to C.M.; FPU grant from the Spanish government (AP2010-5594) to B.F.-C.

REFERENCES

Barnes, C., Maxwell, D., Reuman, D. C. and Jennings, S. (2010) Global patterns in predator-prey size relationships reveal size dependency of trophic transfer efficiency. *Ecology*, **91**, 222–232.

Basedow, S. L., Tande, K. S. and Zhou, M. (2010) Biovolume spectrum theories applied: spatial patterns of trophic levels within a mesozooplankton community at the polar front. *J. Plankton Res.*, **32**, 1105–1119.

Behrenfeld, M. J., O'Malley, R. T., Siegel, D. A., McClain, C. L., Sarmiento, J. L., Feldman, G. C., Milligan, A. J. and Falkowski, P. G. *et al.* (2006) Climate-driven trends in contemporary ocean productivity. *Nature*, **444**, 752–755.

Benavides, M., Moisander, P. H., Daley, M. C., Bode, A. and Arístegui, J. (2016) Longitudinal variability of diazotroph abundances in the subtropical North Atlantic Ocean. *J. Plankton Res.*, **38**, 662–672.

Blanco, J. M., Echevarria, F. and Garcia, C. M. (1994) Dealing with size spectra: some conceptual and mathematical problems. *Sci. Mar.*, **58**, 17–29.

Bode, A., Alvarez-Ossorio, M. T., Cunha, M. E., Garrido, S., Peleteiro, J. B., Porteiro, C., Valdés, L. and Varela, M. (2007) Stable nitrogen isotope studies of the pelagic food web on the Atlantic shelf of the Iberian Peninsula. *Prog. Oceanogr.*, **74**, 115–131.

Bowen, G. (2010) Isoscapes: spatial pattern in isotopic biogeochemistry. *Annu. Rev. Earth Planet. Sci.*, **38**, 161–187.

Capone, D. G., Burns, J. A., Montoya, J. P., Subramaniam, A., Mahaffey, C., Gunderson, T., Michaels, A. F. and Carpenter, E. J. (2005) Nitrogen fixation by *Trichodesmium* spp.: an important source of new nitrogen to the tropical and subtropical North Atlantic Ocean. *Glob. Biogeochem. Cycles*, **19**, doi:10.1029/2004GB002331.

Chassot, E., Mélin, F., Le Pape, O. and Gascuel, D. (2007) Bottom-up control regulates fisheries production at the scale of eco-regions in European seas. *Mar. Ecol. Prog. Ser.*, **343**, 45–55.

Chust, G., Allen, J. I., Bopp, L., Schrum, C., Holt, J., Tsiaras, K., Zavatarelli, M. and Chifflet, M. *et al.* (2014) Biomass changes and trophic amplification of plankton in a warmer ocean. *GCB Bioenergy*, doi:10.1111/gcb.12562.

Coplen, T. B. (2011) Guidelines and recommended terms for expression of stable isotope-ratio and gas-ratio measurement results. *Rapid Commun. Mass Spectrom.*, **25**, 2538–2560.

Duce, R. A., Laroche, J., Altieri, K., Arrigo, K. R., Baker, A. R., Capone, D. G., Cornell, S. and Dentener, F. *et al.* (2008) Impacts of atmospheric anthropogenic nitrogen on the open ocean. *Science*, **320**, 893–897.

Fernández, A., Mouriño-Carballido, B., Bode, A., Varela, M. and Marañón, E. (2010) Latitudinal distribution of *Trichodesmium* spp. and N_2 fixation in the Atlantic Ocean. *Biogeosciences*, **7**, 3167–3176.

Fernández-Castro, B., Mouriño-Carballido, B., Marañón, E., Chouciño, P., Gago, J., Ramírez, T., Vidal, M. and Bode, A. *et al.* (2015) Importance of salt fingering for new nitrogen supply in the oligotrophic ocean. *Nat. Geosci.*, **6**, doi:10.1038/ncomms9002.

Fry, B. and Quiñones, R. B. (1994) Biomass spectra and stable isotope indicators of trophic level in zooplankton of the northwest Atlantic. *Mar. Ecol. Prog. Ser.*, **112**, 201–204.

Gutiérrez-Rodríguez, A., Décima, M., Popp, B. N. and Landry, M. R. (2014) Isotopic invisibility of protozoan trophic steps in marine food webs. *Limnol. Oceanogr.*, **59**, 1590–1598.

Hauss, H., Franz, J. M. S., Hansen, T., Struck, U. and Sommer, U. (2013) Relative inputs of upwelled and atmospheric nitrogen to the eastern tropical North Atlantic food web: spatial distribution of $\delta^{15}N$ in mesozooplankton and relation to dissolved nutrient dynamics. *Deep-Sea Res.*, **75**, 135–145.

Hunt, B. P. V., Allain, V., Menkes, C., Lorrain, A., Graham, B., Rodier, M., Pagano, M. and Carlotti, F. (2015) A coupled stable isotope-size spectrum approach to understanding pelagic food-web dynamics: a case study from the southwest sub-tropical Pacific. *Deep Sea Res. II*, **113**, 208–224.

Jennings, S., Maxwell, T. A. D., Schratzberger, M. and Milligan, S. P. (2008) Body-size dependent temporal variations in nitrogen stable isotope ratios in food webs. *Mar. Ecol. Prog. Ser.*, **370**, 199–206.

Jennings, S., Pinnegar, J. K., Polunin, N. V. C. and Boon, T. W. (2001) Weak cross-species relationships between body size and trophic level belie powerful size-based trophic structuring in fish communities. *J. Anim. Ecol.*, **70**, 934–944.

Kaufman, Y. J., Koren, I., Remer, L. A., Tanré, D., Ginoux, P. and Fan, S. (2005) Dust transport and deposition observed from the Terra-Moderate Resolution Imaging Spectroradiometer (MODIS) spacecraft over the Atlantic Ocean. *J. Geophys. Res.*, **110**, doi:10.1029/2003JD004436.

Landrum, J. P., Altabet, M. A. and Montoya, J. P. (2011) Basin-scale distributions of stable nitrogen isotopes in the subtropical North Atlantic Ocean: contribution of diazotroph nitrogen to particulate organic matter and mesozooplankton. *Deep Sea Res.*, **58**, 615–625.

Legendre, L. and Le Fèvre, J. (1995) Microbial food webs and the export of biogenic carbon in oceans. *Aquat. Microb. Ecol.*, **9**, 69–77.

Longhurst, A.R. (2007) *Ecological Geography of the Sea*, 2nd edn.(Elsevier, Amsterdam.

Marañón, E. (2009) Phytoplankton size structure. In: Steele, J. H., Turekian, K. K. and Thorpe, S. A. (eds), *Encyclopedia of Ocean Sciences*, 2nd edn.(Academic Press, Oxford pp. 4249–4256.

McMahon, K. W., Hamady, L. L. and Thorrold, S. R. (2013) Ocean ecogeochemistry: a review. *Oceanogr. Mar. Biol. Annu. Rev.*, **51**, 327–374.

Molina-Ramírez, A., Cáceres, C., Romero-Romero, S., Bueno, J., González-Gordillo, J. I., Irigoien, X., Sostres, J. and Bode, A. *et al.* (2015) Functional differences in the allometry of the water, carbon and nitrogen content of gelatinous organisms. *J. Plankton Res.*, **37**, 989–1000.

Mompeán, C., Bode, A., Benítez-Barrios, V. M., Domínguez-Yanes, J. F., Escánez, J. and Fraile-Nuez, E. (2013) Spatial patterns of plankton biomass and stable isotopes reflect the influence of the nitrogen-fixer *Trichodesmium* along the subtropical North Atlantic. *J. Plankton Res.*, **35**, 513–525.

Moore, C. M., Mills, M. M., Achterberg, E. P., Geider, R. J., Laroche, J., Lucas, M. I., McDonagh, E. L. and Pan, X. *et al.* (2009) Large-scale distribution of Atlantic nitrogen fixation controlled by iron availability. *Nat. Geosci.*, **2**, 867–871.

Moreno-Ostos, E.(ed.) (2012) Expedición de circunnavegación Malaspina 2010. Cambio global y exploración de la biodiversidad del océano. *Libro blanco de métodos y técnicas de trabajo oceanográfico*. Consejo Superior de Investigaciones Científicas (CSIC), Madrid.

Morin, S., Savarino, J., Frey, M. M., Domine, F., Jacobi, H. W., Kaleschke, L. and Martins, J. M. F. (2009) Comprehensive isotopic composition of atmospheric nitrate in the Atlantic Ocean boundary layer from 65°S to 79° N. *J. Geophys. Res. (D Atmos.)*, **114**, doi:10.1029/2008JD010696.

Mouriño, B., Fernández, E. and Alves, M. (2004) Thermohaline structure, ageostrophic vertical velocity fields and phytoplankton distribution and production in the northeast Atlantic subtropical front. *J. Geophys. Res.*, **109**, doi:10.1029/2003JC001990.

Mouriño-Carballido, B., Graña, R., Fernández, A., Bode, A., Varela, M., Domínguez, J. F., Escánez, J. and De Armas, D. *et al.* (2011) Importance of N_2 fixation vs. nitrate eddy diffusion along a latitudinal transect in the Atlantic Ocean. *Limnol. Oceanogr.*, **56**, 999–1007.

Mulholland, M. R. (2007) The fate of nitrogen fixed by diazotrophs in the ocean. *Biogeosciences*, **4**, 37–51.

Oschlies, A. and Garçon, V. (1998) Eddy-induced enhancement of primary production in a model of the North Atlantic Ocean. *Nature*, **394**, 266–269.

Piontkovski, S. A., Landry, M. R., Finenko, Z. Z., Kovalev, A. V., Williams, R., Gallienne, C. P., Mishonov, A. V. and Skryabin, V. A. *et al.* (2003) Plankton communities of the South Atlantic anticyclonic gyre. *Oceanol. Acta*, **26**, 255–268.

Platt, T. and Denman, K. (1978) The structure of pelagic marine ecosystems. *Rapp. P.-v. Réun. Cons. int. Explor. Mer*, **173**, 60–65.

Post, D. M. (2002) Using stable isotopes to estimate trophic position: models, methods, and assumptions. *Ecology*, **83**, 703–718.

Poulin, F.J. and Franks, P.J.S. (2010) Size-structured planktonic ecosystems: constraints, controls and assembly instructions. *J. Plankton Res.*, **32**, 1121–1130.

Quiñones, R., Platt, T. and Rodriguez, J. (2003) Patterns of biomass-size spectra from oligotrophic waters of the Northwest Atlantic. *Prog. Oceanogr.*, **57**, 405–427.

Rangel, T. F. L. V. B., Diniz-Filho, J. A. F. and Bini, L. M. (2010) SAM: a comprehensive application for spatial analysis in macroecology. *Ecography*, **33**, 46–50.

Rangel, T. F. L. V. B., Field, R. and Diniz-Filho, J .A. F. (2011) *SAM tutorial.* International Biogeographic Society Meeting, Crete.

Richardson, A. J. and Schoeman, D. S. (2004) Climate impact on plankton ecosystems in the Northeast Atlantic. *Science*, **305**, 1609–1612.

Rodriguez, J. and Mullin, M. M. (1986) Relation between biomass and body weight of plankton in a steady state oceanic ecosystem. *Limnol. Oceanogr.*, **31**, 361–370.

Rolff, C. (2000) Seasonal variation in $\delta^{13}C$ and $\delta^{15}N$ of size-fractionated plankton at a coastal station in the northern Baltic proper. *Mar. Ecol. Prog. Ser.*, **203**, 47–65.

San Martin, E., Irigoien, X., Harris, R. P., Lopez-Urrutia, A., Zubkov, M. V. and Heywood, J. L. (2006) Variation in the transfer of energy in marine plankton along a productivity gradient in the Atlantic Ocean. *Limnol. Oceanogr.*, **51**, 2084–2091.

Sommer, U., Stibor, H., Katechakis, A., Sommer, F. and Hansen, T. (2002) Pelagic food web configurations at different levels of nutrient richness and their implications for the ratio fish production:primary production. *Hydrobiologia*, **484**, 11–20.

Søreide, J. E., Tamelander, T., Hop, H., Hobson, K. A. and Johansen, I. (2007) Sample preparation effects on stable C and N isotope values: a comparison of methods in arctic marine food web studies. *Mar. Ecol. Prog. Ser.*, **328**, 17–28.

Torres-Valdes, S., Roussenov, V. M., Sanders, R., Reynolds, S., Pan, X., Mather, R., Landolfi, A. and Wolff, G. A. *et al* (2009) Distribution of dissolved organic nutrients and their effect on export production over the Atlantic Ocean. *Glob. Biogeochem. Cycles*, **23**, doi:10.1029/2008GB003389.

Vanderklift, M. A. and Ponsard, S. (2003) Sources of variation in consumer-diet $\delta^{15}N$enrichment: a meta-analysis. *Oecologia*, **136**, 169–182.

Ward, B. A., Dutkiewicz, S. and Follows, M. J. (2014) Modelling spatial and temporal patterns in size-structured marine plankton communities: top-down and bottom-up controls. *J. Plankton Res.*, **36**, 31–47.

Zhou, M. (2006) What determines the slope of a plankton biomass spectrum?. *J. Plankton Res.*, **28**, 437–448.